analytical chemistry

Article

pubs.acs.org/ac

^{15}N-NMR-Based Approach for Amino Acids-Based ^{13}C-Metabolic Flux Analysis of Metabolism

Pierre Millard, Edern Cahoreau, Maud Heuillet, Jean-Charles Portais, and Guy Lippens*

LISBP, Université de Toulouse, CNRS, INRA, INSA, 31077, Toulouse, France

Supporting Information

ABSTRACT: NMR analysis of the isotope incorporation in amino acids can be used to derive information about the topology and operation of cellular metabolism. Although traditionally performed by ^{1}H and/or ^{13}C NMR, we present here novel experiments that exploit the ^{15}N nucleus to derive the same information with increased efficiency. Combined with a novel Hα-^{13}CO experiment, we increase the coverage of the isotopic space that can be probed by obtaining the complete distribution of isotopic species for the first two carbons of amino acids in cellular biomass hydrolysates. Our approach was evaluated using as reference material a biologically produced sample containing ^{15}N-labeled metabolites with fully predictable ^{13}C-labeling patterns. Results show excellent agreement between measured and expected isotopomer abundances for the different NMR experiments, with an accuracy and precision within 1%. We also demonstrate how these experiments can give detailed information about metabolic fluxes depending on the expression level of a critical enzyme. Hence, exploiting the ^{15}N labeling of a cellular sample accelerates subsequent analysis of the hydrolyzed biomass and increases the coverage of isotopomers that can be quantified, making it a promising tool to increase the throughput and the resolution of ^{13}C-fluxomics studies.

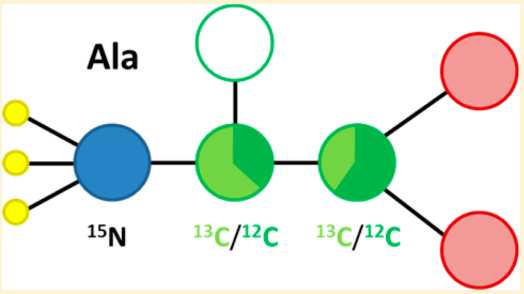

Fluxomics aims at elucidating the topology and operation of metabolic networks by observing the ^{13}C incorporation in different metabolites after growing cells on a ^{13}C labeled substrate.[1−7] One widespread strategy is to focus on how the different amino acids incorporate the ^{13}C label and thereby rely on the quantification of their different isotopomers (isotopic isomers). Free amino acids, protein derived amino acids, or the total pool can be analyzed. The latter can be obtained by total hydrolysis of the full sample, thereby providing abundant material for the analysis. Typical NMR techniques for isotopomer quantification are based on nondecoupled homonuclear experiments such as the TOCSY experiment,[8,9] but J-resolved heteronuclear experiments have equally been proposed.[3,10] Nevertheless, the experiments suffer from several drawbacks: overlap specifically of the Hα protons can be severe; in order to be quantitative, long relaxation delays are necessary to cancel out the effect of the different relaxation properties of ^{12}C/^{13}C bound protons; carbonyl carbons are inaccessible as they have no attached proton.

Although the ^{15}N nucleus has been incorporated in several tags for metabolite identification,[11,12] most NMR studies in the fields of metabolomics or fluxomics rely on ^{1}H and ^{13}C NMR. In protein NMR, most experiments exploit the favorable dispersion of the amide ^{15}N frequency, making the ^{1}H, ^{15}N HSQC the workhorse of the myriad of n-dimensional NMR experiments for structural and dynamic protein analysis.[13] However, in the majority of these latter experiments, only chemical shifts are looked for, whereas quantification is of less importance.

We explore here how ^{15}N-based NMR experiments can be used in the field of fluxomics, where quantification is of prime importance, and show that they overcome some of the aforementioned shortcomings of NMR. First, we show that the HISQC-TOCSY and HNCA experiments can be adapted to quantify the specific enrichment of Cα and the fractional ^{13}CO incorporation for amino acids with a ^{13}Cα, respectively. Combined with a HACO experiment, they allow one to quantify the four isotopic species of the (Cα-CO) block of amino acids. This approach was validated using a biologically produced ^{13}C standard isotopic sample with equal proportions of each isotopic species.

As a proof of concept of their biological applicability, the proposed experiments were used to quantify the control exerted by the first enzyme of the pentose phosphate pathway (G6PDH) on the glycolytic and pentose phosphate flux in *Escherichia coli*. Estimation of these fluxes was based on the absolute quantification of the four isotopic species for the (Cα, CO) two-carbon block of leucine, that derives from the acetyl moiety of acetyl-coA (AcCoA) (Figure 1).

EXPERIMENTAL SECTION

Organisms and Cultures. Wild-type *Escherichia coli* K-12 MG1655 and its derivative mutants (Pzwf1.1, Pzwf1.3, and Pzwf.3) with gradual expression of the *zwf* gene encoding the

Received: December 1, 2016
Accepted: January 9, 2017
Published: January 9, 2017

DOI: 10.1021/acs.analchem.6b04767
Anal. Chem. 2017, 89, 2101−2106

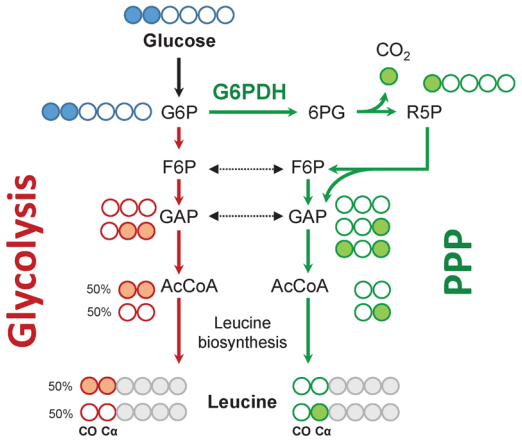

Figure 1. Simplified network of the glycolytic (red) and pentose phosphate (PPP, green) pathways of *E. coli*, showing ^{13}C labeling patterns of some metabolic intermediates and leucine when 1,2-$^{13}C_2$-glucose is used as label input. Empty (filled) circles represent ^{12}C (^{13}C) atoms, and gray circles represent either ^{12}C or ^{13}C atoms.

glucose-6-phosphate dehydrogenase (G6PDH) were used in all physiological experiments.[14] Strains were grown on M9 minimal medium containing 5 mM KH_2PO_4, 10 mM Na_2HPO_4, 9 mM NaCl, 40 mM $^{15}NH_4Cl$, 0.8 mM $MgSO_4$, 0.1 mM $CaCl_2$, 0.3 mM thiamine, and 15 mM glucose or 45 mM acetate as unique carbon source. ^{12}C-glucose and ^{12}C-acetate were obtained from Sigma-Aldrich (St. Louis, MO, USA). 1,2-$^{13}C_2$- and U-$^{13}C_6$-glucose and 1-^{13}C-, 2-^{13}C-, and U-^{13}C-acetate were obtained from Eurisotop (St. Aubin, France). Glucose, acetate, and thiamine were sterilized by filtration; the other compounds were autoclaved separately. Batch cultures were carried out in 500 mL baffled flasks (37 °C, 200 rpm) with 50 mL of medium. Cell growth was monitored by measuring optical density at 600 nm with a Genesys 6 spectrophotometer (Thermo, Carlsbad, CA, USA).

Analysis of ^{13}C-Labeled Acetate by NMR. The ^{13}C-acetate mixture used as label input for the production of the Pascal Triangle (PT) sample contains the four isotopic species of acetate in equal proportions, as previously described for the preparation of a mass spectrometry standard.[15] The proportions of each acetate form were measured by 1D ^1H NMR on a Bruker Avance 500 MHz spectrometer (Bruker, Rheinstetten, Germany) equipped with a 5 mm z-gradient BBI probe head, using a *zgpr30* sequence with a relaxation delay of 20 s, at a temperature of 298 K. A total of 64 scans were accumulated (64k points with a spectral width of 10 ppm) after 8 dummy scans. The experimental distribution of isotopic species (^{12}C-acetate: 25.0 ± 0.5%; 1-^{13}C-acetate: 25.0 ± 0.5%; 2-^{13}C-acetate: 25.2 ± 0.5%; U-^{13}C-acetate: 24.8 ± 0.5%) corresponds to a molecular ^{13}C-enrichment of 49.9 ± 0.7%.

Sample Preparation for NMR Analyses. The ^{15}N, ^{13}C algal extract (Cambridge Isotope Laboratories, Andover, USA) was further hydrolyzed in 6 N HCl (12 h at 100 °C) and dried by evaporation. Bacterial samples containing 15 mg of biomass were collected in mid-exponential growth phase. After centrifugation, the pellet was hydrolyzed in 6 N HCl (12 h at 100 °C) and dried by evaporation. All hydrolysates were resuspended in 200 μL of H_2O with 0.1% HCl and introduced in a 3 mm tube. This tube was inserted in a 5 mm regular NMR tube filled with D_2O for locking purposes and 10 mM TMSP for proton referencing.

NMR Experiments. NMR experiments were performed on a Bruker Avance III 800 MHz spectrometer equipped with a QCI-P cryogenic probe head. Analyses were performed at 273.2 K. Spectra were acquired and processed using the Bruker Topspin 3.0 software. Details of all pulse sequences and protocols used for data analysis are given in the Supporting Information.

^{13}C-Metabolic Flux Analyses. A targeted ^{13}C-metabolic flux analysis experiment was designed to quantify the flux partition between glycolysis and the pentose phosphate pathway (PPP) in four *E. coli* strains with gradual expression of the *zwf* gene.[14] This latter gene encodes the glucose-6-phosphate dehydrogenase (G6PDH) enzyme, which catalyzes the first step of the PPP. Cells were grown in minimal medium containing 1,2-$^{13}C_2$-glucose and $^{15}NH_4^+$ as sole carbon and nitrogen sources, respectively, and the ^{13}C-incorporation into proteinogenic amino acids was measured using the HNCA, HISQC-TOCSY, and HACO-DIPSY experiments.

Estimation of the PPP and glycolytic fluxes was based on the absolute quantification of the four isotopic species for the (Cα, CO) two-carbon block of leucine, which derives from the acetyl moiety of acetylcoA (AcCoA) (Figure 1). 1,2-$^{13}C_2$-glucose metabolized through glycolysis forms unlabeled and fully labeled AcCoA in equal proportions. In contrast, C_1-decarboxylation of glucose through the oxidative branch of the PPP and carbon scrambling through its nonoxidative branch produce unlabeled and singly labeled AcCoA. The relative fluxes through glycolysis and PPP were thus estimated from the fraction of fully labeled CO-Cα-leucine, using the following algebraic equations:

$$\text{glycolysis} = 2 \times \text{Leu}_{11xxxx}$$

$$\text{PPP} = 2 \times (0.5 - \text{Leu}_{11xxxx})$$

The precision of the estimated fluxes was derived from the precision of NMR measurements (standard deviation of 1%).

RESULTS AND DISCUSSION

^{15}N-Based NMR Experiments for Quantitative ^{13}C-Isotopic Analyses. To start our analysis, we have to recognize that the amino acids after complete hydrolysis of the cellular content by overnight incubation at 100 °C in 6 N HCl will be present as free amino acids exhibiting the NH_3^+ group of a primary amine. Similar to the NH_3^+ side chain of the lysine, the nitrogen frequency values of primary amines in unprotected amino acids are expected to be in the 30−40 ppm range, unlike the backbone amide nitrogen spins that resonate at 105−125 ppm. Moreover, the free amine protons are subject to rapid exchange with water. This latter problem is less severe at the acidic pH, that is maintained even after evaporation of the HCl, and can be further reduced by measuring at low temperature. Avoiding magnetization terms of the form $I_zN_{x/y}$ that suffer from exchange with water by favoring pure nitrogen $N_{x/y}$ terms, as implemented in the HISQC sequence (Figure S1),[16] yields sharper signals in the ^{15}N dimension than the conventional HSQC spectra (Figure 2). Finally, separating the D_2O required for field locking from the aqueous sample by using a 3 mm tube containing only H_2O inside a 5 mm tube filled with D_2O further avoids the isotope effect of the deuterium on the ^{15}N nucleus.[16] Taking into account these different factors, the resulting HISQC spectrum of a $^{13}C/^{15}N$ labeled algal hydrolysate yields a high quality spectrum, in which at least 12 individual resonances can be distinguished (Figure 2). On

DOI: 10.1021/acs.analchem.6b04767
Anal. Chem. 2017, 89, 2101−2106

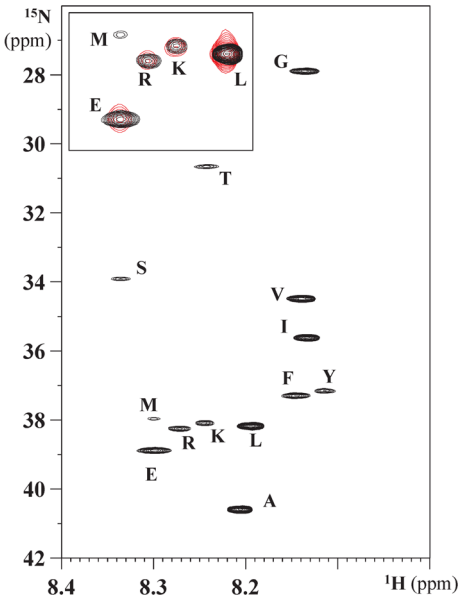

Figure 2. Assigned ^{1}H, ^{15}N HISQC spectrum of the $^{13}C/^{15}N$ labeled algal extract after complete hydrolysis. The inset compares the HISQC spectrum (black) with the HSQC spectrum (red) of the same sample acquired and processed with identical parameters.

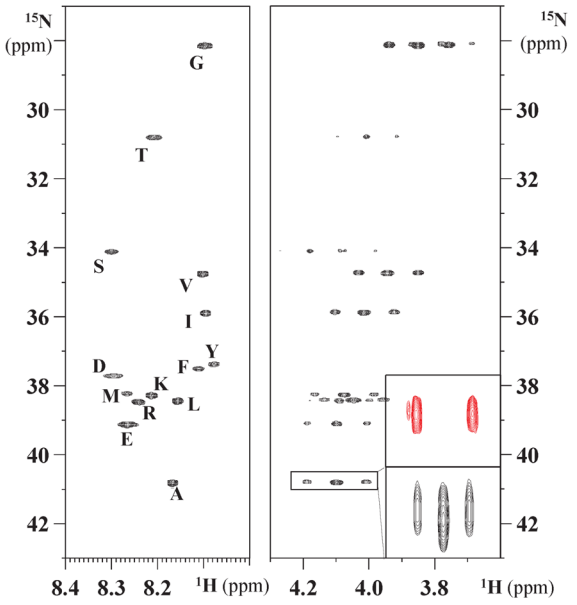

Figure 3. (Left) Annotated HISQC spectrum of the U-^{15}N PT-^{13}C labeled bacterial hydrolysate. (Right) Hα region of the HISQC-TOCSY experiment without ^{13}C decoupling in the direct dimension. The inset shows the Ala correlation peak in the U-^{13}C labeled sample (red) or in the PT-^{13}C sample (black), with a slight upfield shift for the ^{15}N frequency of the unlabeled ($^{12}C\alpha$) to labeled ($^{13}C\alpha$) forms. The relative integral of the central line (Hα-$^{12}C\alpha$) to the sum of the satellites (Hα-$^{13}C\alpha$) gives the ratio of $^{12}C\alpha/^{13}C\alpha$. For sake of clarity, results are expressed as the proportion of ^{13}C atoms at a particular position relative to the total pool of isotopomers for the given amino acid (i.e., the ratio $^{13}C\alpha/(^{12}C\alpha + {}^{13}C\alpha)$.

the basis of a TOCSY-HISQC experiment in combination with a slightly modified HNCACB triple resonance experiment, one can assign these resonances, resulting in unambiguous assignment of the spectrum (Figure S2).

To explore the possibilities of this ^{1}H, ^{15}N HISQC spectrum of measuring ^{13}C incorporation in the different amino acids, we prepared two samples of *Escherichia coli* K-12 bacteria with uniform ^{15}N labeling. The first one was grown with U-^{13}C glucose as the sole carbon source, leading to uniform ^{13}C incorporation at all carbon positions. The second one was grown on equimolar concentrations of the four isotopic species of acetate (as verified by 1D ^{1}H NMR; see the Experimental Section), leading to a 50% probability of carbon incorporation at every position in all amino acids (PT sample).[15] We hydrolyzed the resulting biomass of both samples with the same procedure and found similar correlation peaks as in the algal hydrolysate, although with slightly different intensities (Figure 3).

In protein spectra, the ^{13}C nucleus has a small isotope effect on the ^{15}N amide frequency, and it proved to be even less for the isolated amino acids (Figure 3), excluding it as a factor to discriminate the $^{12}C\alpha$ and $^{13}C\alpha$ labeled amino acids. We therefore implemented a HISQC-TOCSY experiment without ^{13}C decoupling in the direct detection. The first advantage of this experiment is the good resolution: in the ^{15}N dimension, even when the experiment is run in a 2D version, and in the direct proton dimension, where we can immediately distinguish the $^{12}C/^{13}C$ coupled Hα protons by their ^{1}J coupling (Figure 3). Equally important, however, is that the experiment starts with the NH_3^+ proton magnetization rather than with the Hα magnetization term. Whereas the relaxation properties of the former are independent of the labeling of the Cα position, the Hα proton can relax differently when coupled to a $^{12}C\alpha$ or $^{13}C\alpha$ nucleus, requiring lengthy relaxation delays (see below). When considering the ratios of $^{12}C\alpha/^{13}C\alpha$ Ala derived from traces through the HISQC-TOCSY planes recorded with different relaxation delays, we note indeed that they are independent of the relaxation delay (Figure S3) and correspond well to the expected specific enrichment of 50% for the PT sample (Table 1).

Evaluation of the absolute $^{13}C/^{12}C$ ratio at the carbonyl position of the different amino acids is a more complex problem in fluxomics. It can be solved for the subpopulation of amino acids where the Cα position incorporates a ^{13}C label.

Table 1. Proportion of ^{13}C Atoms at a Particular Position (Relative to the Total Pool of Isotopic Species That Are Measured)[a]

amino acid	$^{13}C\alpha$	^{13}CO ($^{13}C\alpha$)	$^{13}C\alpha$ (^{13}CO)
Ala	49.7 ± 0.8	50.4 ± 0.4	49.8 ± 0.2
Leu	49.4 ± 0.2	50.6 ± 0.3	48.5 ± 0.2
Glu	49.2 ± 0.5	50.4	50.3 ± 0.5
Ile	49.2 ± 0.3	49.2 ± 0.7	48.7 ± 0.6
Val	48.0 ± 0.7	50.2 ± 0.9	48.1 ± 0.4
Gly	49.8 ± 0.7	49.7 ± 0.2	48.3 ± 0.4
Thr	48.2 ± 1.1	49.2 ± 1.0	49.2 ± 0.8

[a]Only those amino acids for which all positions could be evaluated in the 2D planes are given. Error bars come from 3 independent experiments. For Glu, there is overlap with Arg in the 2D H(N)CA plane; thus, the value extracted from the 3D spectrum is given without an error bar. The full data sets are given in the Supporting Information. The $^{13}C\alpha$ content (column 2) was obtained from the HISQC-TOCSY experiment (Figure 3). The ^{13}CO content for the $^{13}C\alpha$ labeled pool (column 3) was obtained from the deconvolution of the traces through the HNCA experiment (Figure 4). Finally, the $^{13}C\alpha$ content for the ^{13}CO labeled pool (column 4) was obtained from the Hα-^{13}CO experiment (Figure 5).

DOI: 10.1021/acs.analchem.6b04767
Anal. Chem. 2017, 89, 2101−2106

Indeed, the ^{1}H, ^{13}C HSQC spectrum allows one to visualize this pool, and omitting carbonyl decoupling during the indirect ^{13}C detection leads to a doublet structure for those ^{13}Cα nuclei that are coupled to a ^{13}CO, whereas a singlet remains for the ^{12}CO bound ^{13}Cα nuclei.[17] Because the Cβ position can equally be labeled or not, the traces through the ^{1}H, ^{13}C HSQC spectrum are generally deconvoluted into their respective components, but the necessary high resolution in the indirect ^{13}C dimension requires a lengthy experiment.

When a ^{15}N label is present, a HNCA spectrum with a good resolution in the ^{13}Cα dimension leads to the same results. Advantages are the possibility to record a reduced window in the carbon dimension (11 ppm), as no nuclei other than the Cα will be excited, and an additional spectral spreading due to the nitrogen frequency when run as a 3D spectrum, allowing the extraction of the ^{13}Cα-^{12}CO versus ^{13}Cα-^{13}CO ratio for all amino acids. As an example, we show the NH_3^+-^{13}Cα correlation for Ala in both U-^{13}C and PT-^{13}C labeled samples with and without ^{13}CO decoupling during the ^{13}Cα evolution, extracted from the 2D H-^{13}Cα planes of the corresponding HNCA spectra (Figure 4). The coupling pattern of the ^{13}Cα

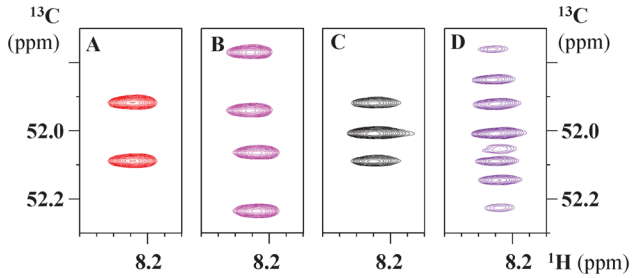

Figure 4. Zoomed in view of the H(N)CA planes representing the Ala Cα resonance in the U-^{13}C (A, B) or PT-^{13}C (C, D) samples with (A, C) or without (B, D) ^{13}CO decoupling during the ^{13}Cα evolution. The ^{13}Cα-^{13}Cβ coupling is active in all spectra for those molecules where the Cβ position is ^{13}C labeled. From the coupling pattern in (D), the (^{13}Cα) ^{13}CO/(^{13}Cα) ^{12}CO ratio can be determined.

can be deconvoluted in terms of populations of ^{13}CO-^{13}Cα-^{13}Cβ, ^{13}CO-^{13}Cα-^{12}Cβ, ^{12}CO-^{13}Cα-^{13}Cβ, and ^{12}CO-^{13}Cα-^{12}Cβ (Figure S4), giving access to the fractional ^{13}CO incorporation for those amino acids with a ^{13}Cα. Together with the measurement of the ^{13}Cα/^{12}Cα ratio from the HISQC spectrum (Figure 3), we thus have the molecular percentage of the ^{13}Cα/^{13}CO and ^{13}Cα/^{12}CO forms for the different amino acids.

Direct assignment of the carbonyl resonances of the labeled amino acids is possible via the HN(CA)CO experiment on the ^{15}N/^{13}C labeled hydrolysate (Figure S5). Omitting the Cα coupling in this experiment to quantify the ^{13}CO nuclei linked to a ^{12}Cα/^{13}Cα is however useless, as the transfer of magnetization strictly requires a ^{13}Cα nucleus; only fully labeled amino acids will hence contribute to the signal. The HN(CA)CO experiment can however be used to assign the carbonyl resonance for the different amino acids (Figure S6). A direct coupling between the carbonyl carbon and the ^{15}N nucleus proved too small to be detectable, but when we recorded the direct ^{13}C spectrum without proton decoupling, we observed a significant broadening of the carbonyl signals. To quantify it, we turned to a sample of U-^{13}C labeled Ala mixed with unlabeled Ala in D_2O and confirmed a direct coupling between the Ala ^{13}CO carbon and its Hα proton (Figure S6). Comparison of the proton spectrum without and with selective ^{13}CO decoupling yielded a coupling constant of 7.3 Hz (Figure S7). This suggests that a direct INEPT transfer between the Hα and carbonyl carbon should be possible, independent of the isotope labeling of the Cα nucleus. When the experiment with Hα selective proton pulses and a suitable delay to refocus the Hα-Hβ coupling was optimized, as was previously proposed in the study of random coil peptides,[18,19] the sequence did yield the expected ^{1}Hα-^{13}CO correlation for the Ala sample (Figure S5). When applied to the ^{15}N/^{13}C labeled bacterial hydrolysate after freeze-drying and resuspension in D_2O, the pulse sequence gave a well-resolved spectrum, in which all Hα-CO correlations could be assigned. After further optimization of the water suppression, we obtained a similar spectrum of the biomass hydrolysate directly in water (Figure 5). Quantifying

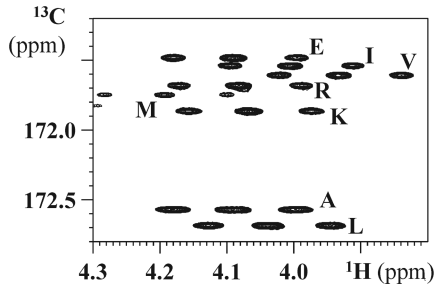

Figure 5. Annotated Hα-^{13}CO spectrum of the U-^{15}N PT-^{13}C labeled bacterial hydrolysate. The absence of ^{13}C decoupling during the proton acquisition allows one to distinguish the ^{12}Cα and ^{13}Cα linked Hα protons for the ^{13}CO labeled amino acids.

the ^{13}C labeled carbonyls in terms of the isotope labeling of the attached Cα nucleus hence becomes possible by omitting the ^{13}Cα decoupling during the direct acquisition while maintaining it during the ^{13}CO indirect evolution.

One pronounced difference of this experiment with the previous ones is that we start with a Hα magnetization term rather than with the NH_3^+ magnetization. Because the dipolar coupling between the Hα and ^{13}Cα nucleus will contribute to the relaxation of this Hα_z term for the ^{13}Cα labeled amino acids, a short relaxation delay will tend to favor the more rapidly relaxing ^{13}Cα population. When varying the relaxation delay between 1 and 6 s, we found only above 5s a stable value that still did not correspond to the expected enrichment of 50%. The origin of the discrepancy was traced to the differential T_2 transverse relaxation of the ^{13}Cα and ^{12}Cα linked Hα magnetization terms, leading this time to an underestimation of the more rapidly relaxing ^{13}Cα linked Hα term (Figure S8). Correcting for this, we do obtain the expected ^{13}Cα enrichment of 50% for the ^{13}CO labeled population of the different amino acids (Table 1).

Quantification of the Four Isotopic Species of the Two-Carbon (Cα-CO) Block of Amino Acids. Because the population of the ^{13}CO nuclei coupled to a ^{13}Cα nucleus in this experiment is the same as the population of the ^{13}Cα nuclei coupled to a ^{13}CO nucleus as previously derived from the H(N)CA plane, we obtain the percentage of ^{13}C atoms in the carbonyl position as the sum of the percentages of the ^{13}CO(^{13}Cα) from the HNCA experiment and the ^{13}CO (^{12}Cα) from the Hα-CO experiment (Figure 6). This completes the data for ^{13}C incorporation at both the Cα and CO position and leads, together with the closure relationship (the sum of the

DOI: 10.1021/acs.analchem.6b04767
Anal. Chem. 2017, 89, 2101−2106

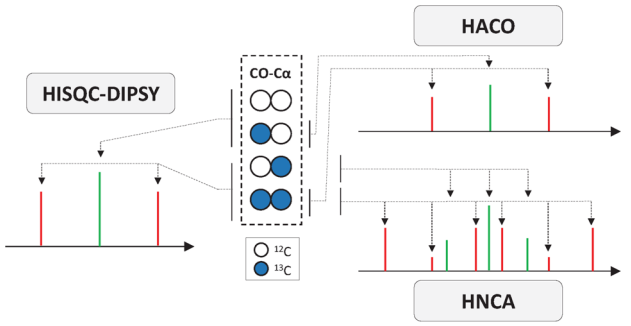

Figure 6. Summary of the information content of the three experiments. For a two-carbon block (Cα-CO), the three independent experiments together with the closure relationship give the quantification of the four isotopic species.

four populations is 100%), to an absolute quantification of the four isotopic species of the two-carbon (Cα-CO) block of the different amino acids (see the Supporting Information for a numerical example).

Application for ^{13}C-Metabolic Flux Analysis. The ^{15}N-based NMR experiments were used to quantify the partitioning of carbon fluxes between glycolysis and the pentose phosphate pathway (PPP) in four *E. coli* strains with gradual expression of the *zwf* gene.[14] This latter gene encodes the glucose-6-phosphate dehydrogenase (G6PDH) enzyme, which catalyzes the first step of the PPP.[20] Cells were grown on 1,2-$^{13}C_2$-glucose as sole carbon source, and fluxes were estimated from the ^{15}N-NMR-based quantification of the four isotopic species of the (Cα, CO) two-carbon block of leucine, as detailed in the Experimental Section. Results show that the PPP flux nonlinearly decreases with decreasing enzyme expression but remains stable when enzyme expression is increased up to 10-fold (Figure 7); G6PDH concentration hence is optimal in the

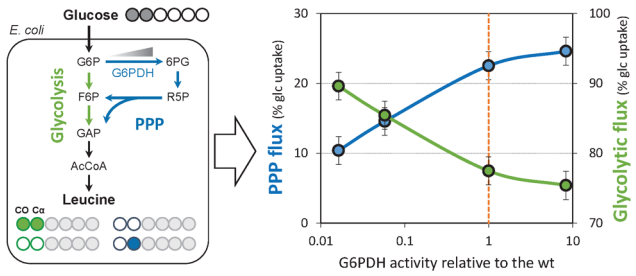

Figure 7. Metabolic fluxes through glycolysis (green dots) and the pentose phosphate pathway (blue dots) as a function of glucose-6-phosphate dehydrogenase (G6PDH) activity. The partitioning of carbon fluxes between glycolysis and the pentose phosphate pathway was quantified from the four (CO, Cα) isotopic species of leucine of *E. coli* cells grown on 1,2-$^{13}C_2$-glucose and $^{15}NH_4^+$ as sole carbon and nitrogen sources, respectively. Filled (empty) circles represent ^{13}C (^{12}C) atoms. Fluxes (±sd) are expressed relative to the glucose uptake rate, and G6PDH activity is relative to the activity measured in the wild-type strain (WT, vertical orange line).

wild-type strain, and a gradual shift of control of this flux partition from gene expression to the metabolic level occurs with increasing enzyme levels.

Using the ^{15}N-based NMR experiments, the ^{13}C-labeling data could be collected within 24 h for the complete set of investigated conditions (3 NMR experiments × 4 strains). Hence, this approach can provide rapidly quantitative insights into changes in metabolism caused by the modulation of enzyme activities. It thereby informs on the underlying flux control mechanisms, an aspect of major interest in the fields of systems biology and metabolic engineering.

CONCLUSION

We have shown that exploiting the ^{15}N labeling of a cellular sample accelerates subsequent analysis of the hydrolyzed biomass in terms of ^{13}C incorporation at the different positions. The proposed experiments can be run as 2D planes in a rapid manner, as they mostly exploit the NH_3^+ magnetization term as starting vector, rely on the good separation of the ^{15}N frequency (Figures 2 and 3), and yield accurate information on the ^{13}C labeling of both the Cα and CO positions for the different amino acids. Together with the Hα-CO experiment, they give access to the absolute quantification of the four isotopic species for the (Cα, CO) two-carbon block of the different amino acids.

We have demonstrated how the proposed ^{15}N-NMR-based approach can be used to accurately quantify the metabolic fluxes and their control in any biological system. Isotopic data derived from a single amino acid were exploited here for targeted ^{13}C-metabolic flux analyses. Of course, additional information on other amino acids can be used in the context of more complete ^{13}C-metabolic flux analyses via detailed modeling approaches. The proposed approach may also provide additional information on N-containing metabolites, which represent a large fraction of the metabolome (e.g., 56% of *E. coli* metabolome contains at least one N atom[21]) and have important biological functions. Finally, the present experiments may be extended following the single-scan 3D-NMR[22] or nonuniform sampling[23] strategies, which have the potential to accelerate further isotopic analyses.

ASSOCIATED CONTENT

Supporting Information

The Supporting Information is available free of charge on the ACS Publications website at DOI: 10.1021/acs.analchem.6b04767.

Sample preparation, mass spectrometry, NMR spectroscopy, data analysis, complete isotopomer determination, flux analysis as a function of G6DPH levels, and supporting figures (PDF)

AUTHOR INFORMATION

Corresponding Author

*Telephone: +33(0)5-61-55-94-92. E-mail: guy.lippens@insa-toulouse.fr.

ORCID

Pierre Millard: 0000-0002-8136-9963

Notes

The authors declare no competing financial interest.

ACKNOWLEDGMENTS

MetaToul (Toulouse metabolomics and fluxomics facilities, www.metatoul.fr) is part of the French National Infrastructure for Metabolomics and Fluxomics MetaboHUB-AR-11-INBS-0010 (www.metabohub.fr) and is supported by the Région Midi-Pyrénées, the ERDF, the SICOVAL, and the French-Minister of Education and Research. All are gratefully acknowledged.

DOI: 10.1021/acs.analchem.6b04767
Anal. Chem. 2017, 89, 2101−2106

REFERENCES

(1) Szyperski, T. *Eur. J. Biochem.* **1995**, *232*, 433−448.
(2) Szyperski, T. *Q. Rev. Biophys.* **1998**, *31*, 41−106.
(3) Massou, S.; Nicolas, C.; Letisse, F.; Portais, J.-C. *Phytochemistry* **2007**, *68*, 2330−2340.
(4) Sekiyama, Y.; Kikuchi, J. *Phytochemistry* **2007**, *68*, 2320−2329.
(5) Fan, T. W.-M.; Lane, A. N. *Prog. Nucl. Magn. Reson. Spectrosc.* **2008**, *52*, 69−117.
(6) Crown, S. B.; Antoniewicz, M. R. *Metab. Eng.* **2013**, *20*, 42−48.
(7) Fan, T. W.-M.; Lane, A. N. *Prog. Nucl. Magn. Reson. Spectrosc.* **2016**, *92*−*93*, 18−53.
(8) Lane, A. N.; Fan, T. W.-M. *Metabolomics* **2007**, *3*, 79−86.
(9) Massou, S.; Nicolas, C.; Letisse, F.; Portais, J.-C. *Metab. Eng.* **2007**, *9*, 252−257.
(10) Kikuchi, J.; Tsuboi, Y.; Komatsu, K.; Gomi, M.; Chikayama, E.; Date, Y. *Anal. Chem.* **2016**, *88*, 659−665.
(11) Tayyari, F.; Gowda, G. A. N.; Gu, H.; Raftery, D. *Anal. Chem.* **2013**, *85*, 8715−8721.
(12) Lane, A. N.; Arumugam, S.; Lorkiewicz, P. K.; Higashi, R. M.; Laulhé, S.; Nantz, M. H.; Moseley, H. N. B.; Fan, T. W.-M. *Magn. Reson. Chem.* **2015**, *53*, 337−343.
(13) Kay, L. E.; Ikura, M.; Tschudin, R.; Bax, A. *J. Magn. Reson.* **1990**, *89*, 496−514.
(14) Heux, S.; Poinot, J.; Massou, S.; Sokol, S.; Portais, J.-C. *Metab. Eng.* **2014**, *25*, 8−19.
(15) Millard, P.; Massou, S.; Portais, J.-C.; Letisse, F. *Anal. Chem.* **2014**, *86*, 10288−10295.
(16) Iwahara, J.; Jung, Y.-S.; Clore, G. M. *J. Am. Chem. Soc.* **2007**, *129*, 2971−2980.
(17) Fan, T. W.-M.; Lane, A. N. *J. Biomol. NMR* **2011**, *49*, 267−280.
(18) Kjaergaard, M.; Brander, S.; Poulsen, F. M. *J. Biomol. NMR* **2011**, *49*, 139−149.
(19) Kjaergaard, M.; Poulsen, F. M. *J. Biomol. NMR* **2011**, *50*, 157−165.
(20) Stincone, A.; Prigione, A.; Cramer, T.; Wamelink, M. M. C.; Campbell, K.; Cheung, E.; Olin-Sandoval, V.; Grüning, N.-M.; Krüger, A.; Tauqeer Alam, M.; et al. *Biol. Rev. Camb. Philos. Soc.* **2015**, *90*, 927−963.
(21) Orth, J. D.; Conrad, T. M.; Na, J.; Lerman, J. A.; Nam, H.; Feist, A. M.; Palsson, B. O. *Mol. Syst. Biol.* **2011**, *7*, 535−543.
(22) Boisseau, R.; Charrier, B.; Massou, S.; Portais, J.-C.; Akoka, S.; Giraudeau, P. *Anal. Chem.* **2013**, *85*, 9751−9757.
(23) Reardon, P. N.; Marean-Reardon, C. L.; Bukovec, M. A.; Coggins, B. E.; Isern, N. G. *Anal. Chem.* **2016**, *88*, 2825−2831.

DOI: 10.1021/acs.analchem.6b04767
Anal. Chem. 2017, 89, 2101−2106